CORRELATION OF WIND TUNNEL AND FLIGHT TEST RESULTS OF A FULL-SCALE HINGELESS ROTOR

Randall L. Peterson
NASA Ames Research Center
Moffett Field, CA

Thomas Maier
Aeroflightdynamics Directorate
U.S. Army Aviation and Troop Command
Moffett Field, CA

Hans Jürgen Langer and Norbert Tränapp
Deutsche Forschungsanstalt für Luft-und Raumfahrt e.V.
Institut für Flugmechanik
Braunschweig, Germany

Abstract

Correlation of wind tunnel results of a full-scale four-bladed hingeless rotor system with flight test measurements is presented. The results presented are from a recently completed full-scale rotor test in the NASA Ames 40- by 80-Foot Wind Tunnel and a recently completed flight test of a BO-105 helicopter at the Deutsche Forschungsanstalt für Luft-und Raumfahrt e.V. (DLR), Braunschweig, Germany. Rotor hub and blade loads are shown over a range of advance ratios from 0.1 to 0.34 for C_T/σ=0.07. Good correlation of measured blade root flap bending moments in the wind tunnel with flight test measurements is shown when the rotor is trimmed to measured flight test hub pitching and rolling moments. Analytical results using the CAMRAD/JA (Comprehensive Analytical Model of Rotorcraft Aerodynamics and Dynamics, Johnson Aeronautics) analysis shows good correlation when the analysis is trimmed to isolated rotor once-per-revolution root flap moments.

Nomenclature

c	blade chord, ft
C_{Mx}/σ	hub rolling moment coefficient, roll moment/$\rho S(\Omega R)^2 R$
C_{My}/σ	hub pitching moment coefficient, pitch moment/$\rho S(\Omega R)^2 R$
C_P/σ	rotor power coefficient, rotor power/$\rho S(\Omega R)^3$
C_T/σ	rotor thrust coefficient, shaft axes, thrust/$\rho S(\Omega R)^2$
P	per rev
R	rotor radius, ft
S	rotor reference area, 4cR, ft^2
V	velocity, ft/sec
α	rotor shaft angle, positive shaft tilt aft, deg
μ	advance ratio, $V/\Omega R$
ρ	air density, $slug/ft^3$
σ	rotor solidity, $S/\pi R^2$
ω_ζ	rotor-blade fundamental inplane bending frequency, rad/sec
Ω	rotor rotation frequency, rad/sec

Presented at the American Helicopter Society Aeromechanics Specialists Conference, San Francisco, California, January 19-21, 1994.

Introduction

The use of wind tunnel test measurements, flight test measurements, and analytical prediction plays a key role in the development of new rotor systems. Such tests are typically performed using a range of rotor system sizes and wind tunnel test facilities. To assure the accuracy of wind tunnel testing methodology, a validation study is in

progress using test results from model- and full-scale tests in comparison with flight test data. This study is being conducted under the auspices of the U.S. Army/German Memorandum of Understanding on Cooperative Research in the Field of Helicopter Aeromechanics. This comparison will allow for a determination of the ability to accurately predict helicopter flight behavior from wind tunnel experiments and the influence of the test facility on these results. Experimental data from a series of wind tunnel tests, including both model- and full-scale experiments, will be studied to determine the extent to which wind tunnel test results can be used to predict flight behavior.

This paper presents the correlation results of a recently completed full-scale test of a BO-105 hingeless rotor in the NASA Ames Research Center 40- by 80-Foot Wind Tunnel with flight test measurements from a recently completed flight test of a BO-105 helicopter at the Deutsche Forschungsanstalt für Luft-und Raumfahrt e.V. (DLR) in Braunschweig Germany. A series of flight tests was conducted at the DLR in the spring and autumn of 1992. These flights were conducted at various altitudes and speeds for steady level flight. Upon completion of the flight test program, the data (Ref. 1) was reduced and evaluated to identify a series of test conditions for the full- and model-scale wind tunnel test programs. The test conditions identified for the full-scale wind tunnel test included five advance ratios (0.1 to 0.34) and two thrust conditions (C_T/σ=0.07 and 0.09). Results presented in this paper are for a nominal 1-g rotor thrust of 5000 lbs (C_T/σ=0.07) and advance ratios from 0.1 to 0.34. Comparisons of wind tunnel and flight test rotor hub moments and blade loading as a function of advance ratio are shown. Also presented in the paper are comparisons between CAMRAD/JA results and measured wind tunnel data. The analytical results are also compared with flight test data.

Test Hardware

Wind Tunnel

The BO-105 helicopter rotor system is a four-bladed, soft inplane ($\omega_\zeta < \Omega$) hingeless rotor with constant chord (0.886 ft), -8 deg linear twist, and a NACA 23012 cambered airfoil. The rotor radius is 16.11 ft; solidity (σ) is 0.07. The rotor hub has 2.5 deg of built-in coning and zero droop or sweep of the blade outboard of the pitch bearing. The BO-105 rotor used in this test was a production rotor set previously used in a flight-test program at Boeing Helicopter. The general characteristics of the main rotor are summarized in Table 1. Additional details about the rotor system are presented in Ref. 2.

Table 1. General characteristics of the BO-105 main rotor.

Type	Hingeless
Radius (ft)	16.11
Number of blades	4
Blade chord (ft)	0.886
Linear blade twist (deg)	-8
Precone (deg)	-2.5
Solidity, σ	0.07
Reference area, S (ft^2)	57.1
Airfoil section	NACA 23012

The BO-105 hingeless rotor was installed on the recently modified Rotor Test Apparatus (RTA). The RTA is a special-purpose drive and support system for operating helicopter rotors in the 40-by 80- and 80- by 120-Foot Wind Tunnels. It houses two electric drive motors, the hydraulic servo-actuators of the primary control-system, and a dynamic control system capable of introducing dynamic perturbations to the non-rotating swashplate (collective and tilt) at frequencies up to 40 Hz. Recent modifications to the RTA include the addition of a five-component balance to measure rotor loads at the hub moment center. This balance was designed and fabricated to measure both the steady and vibratory rotor normal, axial and side forces, together with rotor pitching and rolling moments to rotor thrust levels of 22,000 lbs. An instrumented flex-coupling measures rotor torque and residual normal force.

Flight Test

The BO-105 aircraft used in the flight test program is one of two BO-105 helicopters at the DLR Institute of Flight Mechanics in Braunschweig, Germany. The BO-105 is 5000 lb gross weight aircraft with a maximum sea level speed of 145 knots. Included on the aircraft was an onboard data acquisition system with a sampling rate of 200 Hz. Data was digitized and stored on a removable hard disk during the flight. The removable hard disk was later used to transfer data to another computer system for post-processing.

Instrumentation

Instrumentation for the wind tunnel test included the five-component rotor balance and instrumented flex-coupling, thirty-seven blade bending and torsional

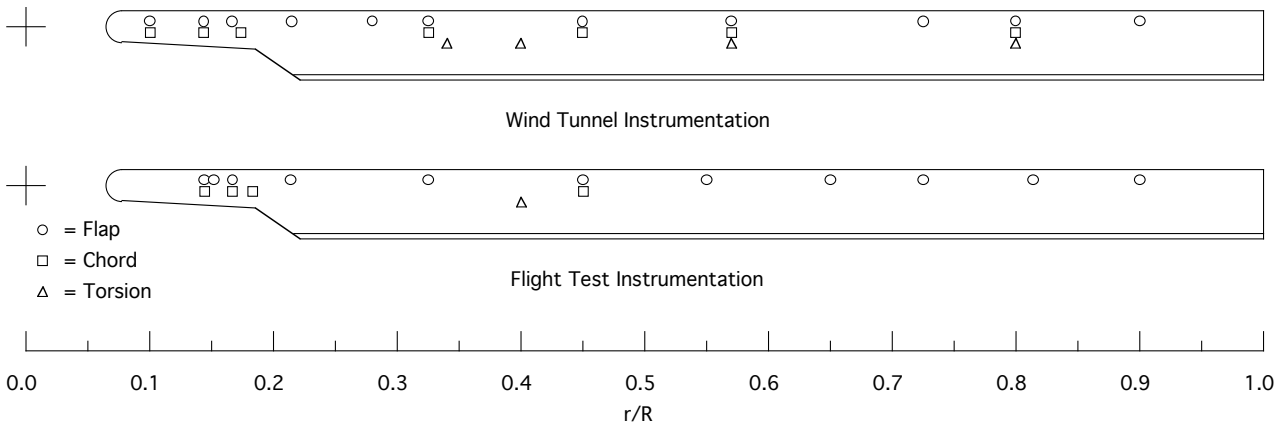

Figure 1. Radial location of flap, chord, and torsion instrumentation for the wind tunnel and flight test programs.

moment measurements (distributed among the four blades), one rotating pitch-link measurement, one blade pitch angle measurement (at the pitch bearing), three stationary control system measurements and standard wind tunnel operating condition measurements.

The flight test instrumentation included pitch, roll and yaw positions and rates, control input displacements, pressure altitude and temperature, climb or descent rate, airspeed, mast moment (main rotor shaft bending) and torque, sixteen blade bending and torsional moment measurements (single blade), two blade pitch angle measurements (at the pitch bearing), and one rotating pitch-link measurement.

A comparison of the blade bending and torsional moment measurement locations between the wind tunnel and the flight test programs are shown in Fig. 1. Identical measurements, on all four blades, at radial stations r/R=0.10 (flap and chord), r/R=0.144 (flap and chord), and r/R=0.40 (torsion) where made in the wind tunnel test program. Blade number one of the wind tunnel test program was composed primarily of the distributed flap bending measurements, while blade number three was composed primarily of the distributed chord bending and torsional moment measurements.

Experimental Programs

Flight Testing

The BO-105 flight tests were performed for level flight only at three different flight (altitude) levels. To get a wide data base for application to the wind tunnel rotor tests, the flight tests were performed for the following conditions; 1) horizontal speed range from hover (OGE) to maximum speed with a stepsize of 10 knots, 2) three different altitudes, 3) two center-of-gravity (c/g) positions (baseline position, and 121 lb mass at the tail), and 4) three different main rotor RPM's in hover (95 percent, 100 percent, and 102 percent).

The horizontal speed stepsize of 10 knots was chosen because previous tests had shown that a stepsize of μ=0.05 (22 knots) is too large for interpolation between data points. Flight testing at different altitudes or flight levels has the effect of increased rotor thrust coefficient with increased altitude to balance the decreasing air density. Results from the flight tests show that rotor thrust coefficient can be varied by 25 percent with a change in altitude. The c/g position was varied by adding mass to the helicopter tail boom. A mass of 121 lb shifts the c/g location by 4.3 inches, which is a 40 percent shift about the allowed range of 7.1 inches for a 5013 lb take-off gross weight. Variation of the c/g position was performed to investigate the influence on control angles and mast bending moments. Three different rotor rotational speeds were set in hover to investigate the influence of tip Mach-numbers on static and dynamic loads.

The primary task for the flight test program was to define test points for a wind tunnel test in the NASA Ames 40- by 80-Foot Wind Tunnel and subsequent testing of a 40 percent scale-model in the German-Dutch Wind Tunnel (DNW). In conducting the flight tests, careful attention to setting up on flight condition was essential. Post test data evaluation was also very important to determine the test conditions for the subsequent wind tunnel tests.

The procedures for setting up on a flight condition were established based on experience from preceding flight tests. Selection of the test points for the subsequent wind tunnel tests required suitable criterion for evaluation of the helicopter trim accuracy. Previous flight tests identified the main disturbance factors that influence steady-state flight as being atmospheric turbulence and control inputs from the pilot. An observation period of the first 3 to 5 rotor revolutions within a data record was found to empirically render the best results to determine the initial trim condition with sufficient suppression of sampling errors due to noise. Some of the criterion used to evaluate the flight test data are summarized as follows; 1) control inputs, both collective and cyclic shall remain constant, 2) the climb or descent rate shall be less than 100 ft/min, 3) the standard deviation of the indicated velocity shall be less than 0.2 knots. The actual tests were conducted with minimal changes to the control inputs and in conditions of low atmospheric turbulence. The best steady-state periodic results for trim were obtained in the speed range of $0.1 \leq \mu \leq 0.25$.

Wind Tunnel Testing

Test conditions in the wind tunnel were obtained by establishing rotor thrust and adjusting cyclic inputs to achieve the fixed-system pitch and roll moments corresponding to the 1P rotating shaft bending measurements on the helicopter, along with the shaft angle and advance ratio as measured in the flight test program. The 1P *Cosine* value corresponds to the hub pitching moment and the 1P *Sine* value corresponds to the hub rolling moment. The collective pitch setting was adjusted to match the aircraft take-off weight minus the fuel burn.

The procedures for setting on a simulated flight condition in the wind tunnel, began first with adjusting the shaft angle of attack, tunnel velocity, rotor thrust and cyclic pitch settings to provide a minimized flap baseline condition at r/R=0.144 on blade number one. The second step was setting rotor rotational speed and then further adjustment of tunnel velocity for the proper advance ratio. The final step was the adjustment of cyclic pitch controls until the real-time numerical display for hub pitching and rolling moments, as measured by the RTA balance, corresponded to the values of the 1P *Cosine* and 1P *Sine* components from the rotating mast moment sensor on the aircraft.

Along with the prescribed hub moment trim data at each simulated flight condition, data was acquired for a minimized flapping condition and for cyclic settings as measured in the flight test. The cyclic control values as measured in the flight test were set using the RTA control console displays resolved from the three fixed-system actuator displacements. This approach was used because a real-time display of the rotating blade pitch angle measurement was unavailable at the time. Resolution of the cyclic inputs as displayed on the RTA control console from the fixed system displacements turns out to be not as accurate as is necessary for these types of comparisons. Therefore, direct comparisons of flight test data with data acquired using the prescribed cyclic approach to setting on condition in the wind tunnel is invalid. A comparison of these three approaches to setting on test conditions in the wind tunnel will be discussed in the next section. No wall corrections have been applied to this data.

Experimental Results

As discussed previously in the paper, the wind tunnel test was conducted with a rotor system having identical measurements on each blade near the root for flap and chord bending (r/R=0.104 and r/R=0.144). Each blade also had an identical torsional moment measurement at r/R=0.40. Figure 2 presents a comparison of oscillatory flap bending at r/R=0.144 for all four blades for a prescribed hub moment trim condition at an advance ratio of μ=0.197. The reasons for these differences, which tend to increase slightly as a function of airspeed, have yet to be fully explained, other than blade-to-blade dissimilarities. Comparisons for chord bending and torsional moments for all four blades, show similar differences between blades and similar trends with advance ratio.

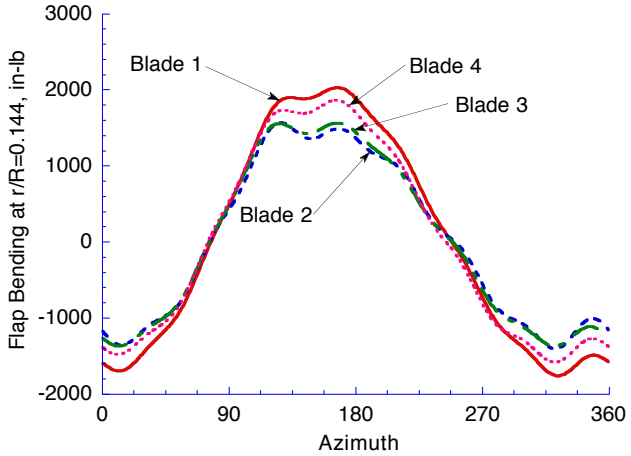

Figure 2. Comparison of oscillatory flap bending for all four blades at r/R=0.144, prescribed hub moment trim, μ=0.197.

Comparisons of data between the wind tunnel and flight test at the blade root will be with the flap and chord bending measurements at r/R=0.144, as this is the measurement station nearest the blade root for the flight test. The comparisons of flap and chord bending at the blade root (r/R=0.144) are made with measurements from blade number three in the wind tunnel. Comparisons of torsional moment are also made with measurements from blade number three. This applies to the comparisons of the three approaches to setting on condition in the tunnel and comparisons between wind tunnel and flight. Blade number three was chosen as the representative blade after careful review of the wind tunnel data relative to the flight test, and correlation with analysis. Comparisons of flap bending near the blade midspan are made with blade number one because no measurement was available on blade number three. Comparisons of chord bending at r/R=0.57 are made with blade number one, while comparisons at r/R=0.45 are made with blade number three.

Comparison of Trim Procedures

Figure 3 is an overall comparison of the hub pitching and rolling moments from the flight test as a function of advance ratio, with data acquired for three different procedures to setting on a test condition in the wind tunnel. The differences between the flight test and the moment trim in the wind tunnel at all advance ratios for both the pitching and rolling moments are primarily due to an error in the calibrated true airspeed of the flight test results at the time of the wind tunnel test. Shortly after completion of the wind tunnel test, it was discovered that the forward speed measurement of the flight test data had not been corrected for the rotor induced flow. This error has the effect of shifting all the wind tunnel trim settings

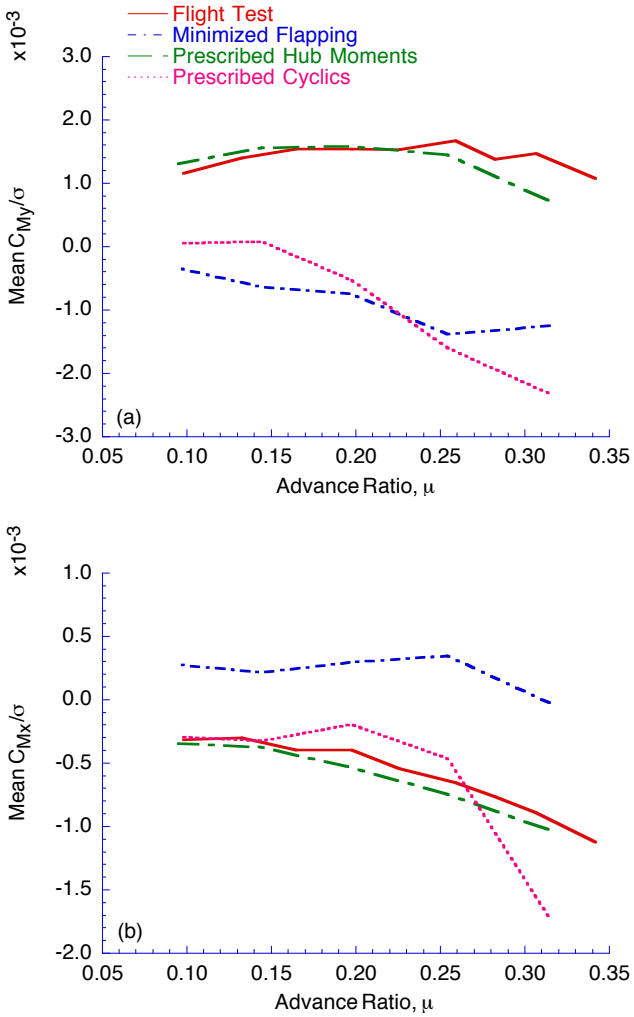

Figure 3. Comparison of measured flight test hub moments with three procedures to setting on a test condition in the wind tunnel, a) hub pitching moment, b) hub rolling moment.

Table 2. Summary of flight test data shown in Fig. 3.

μ	α	C_T/σ	C_{Mx}/σ	C_{My}/σ
0.098	-2.6°	0.071	-0.00031	0.00116
0.132	-2.7°	0.071	-0.00030	0.00141
0.164	-3.3°	0.071	-0.00039	0.00155
0.197	-4.0°	0.071	-0.00039	0.00155
0.225	-4.8°	0.072	-0.00054	0.00154
0.259	-5.6°	0.072	-0.00065	0.00168
0.282	-7.2°	0.071	-0.00076	0.00138
0.306	-7.7°	0.071	-0.00089	0.00148
0.341	-9.6°	0.072	-0.00112	0.00109

to a corresponding lower advance ratio relative to the flight data. Despite these differences, the ability to set up

Table 3. Summary of wind tunnel data for prescribed hub moment trim shown in Fig. 3.

μ	α	C_T/σ	C_{Mx}/σ	C_{My}/σ
0.095	-2.5°	0.071	-0.00034	0.00132
0.144	-3.3°	0.072	-0.00037	0.00157
0.197	-4.8°	0.071	-0.00053	0.00159
0.253	-7.1°	0.073	-0.00074	0.00146
0.313	-9.6°	0.071	-0.00102	0.00074

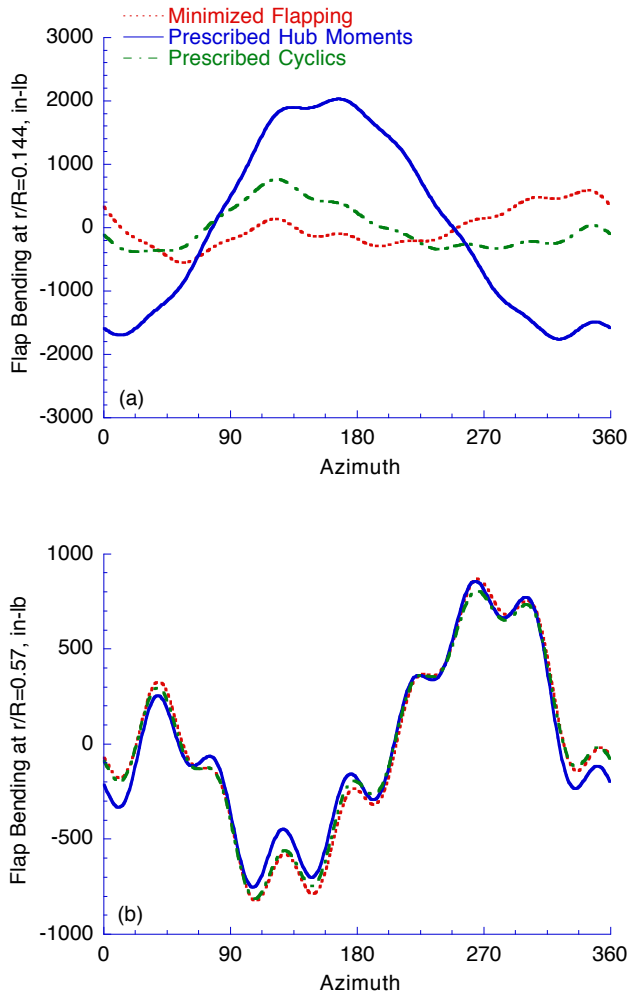

Figure 4. Comparison of oscillatory flap bending moments with three procedures to setting on a test condition in the wind tunnel, a) flap bending at r/R=0.144, b) flap bending at r/R=0.57.

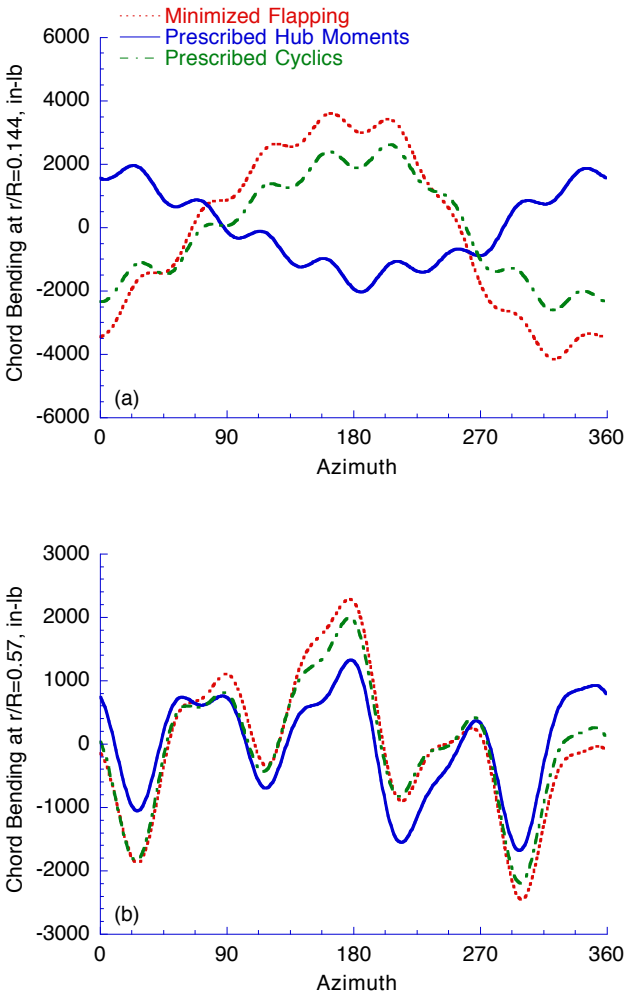

Figure 5. Comparison of oscillatory chord bending moments with three procedures to setting on a test condition in the wind tunnel, a) chord bending at r/R=0.144, b) chord bending at r/R=0.57.

on the flight test hub pitching and rolling moments using the RTA balance was successfully demonstrated in this test program (Fig. 3). Additionally, large differences between flight test and wind tunnel prescribed hub moment trim is noted in Fig. 3a for advance ratios of $\mu \geq 0.3$. This is attributed to unsteadiness of the rotor in the tunnel at these speeds. The data presented in Fig. 3 is summarized in Tables 2 and 3. The data from the flight test program is presented in Table 2, while Table 3 summarizes the data acquired for the prescribed hub moment trim procedure in the wind tunnel.

Figures 4-6 present detailed oscillatory time histories (1-8 harmonics) for flap and chord bending and torsional moment at several blade radial stations for the three different approaches to setting on a test condition in the wind tunnel. The results presented are for 1-g thrust ($C_T/\sigma=0.07$) at an advance ratio of $\mu=0.197$ and a shaft angle of $\alpha=-4.8$ deg. Figure 4 is a comparison of oscillatory flap bending moment time histories at two blade radial locations (r/R=0.144 and r/R=0.57). Distinct differences are noted at the inboard radial station (r/R=0.144), between the procedure for setting up on prescribed hub moments and the procedures for minimized flapping or prescribed cyclics. These differences are almost entirely a function of the 1P control input for trim. The higher frequency loading (2P-8P) is basically unchanged as a function of the trim procedure. Small differences in the measured flap bending moment are noted at the midspan (r/R=0.57) radial station.

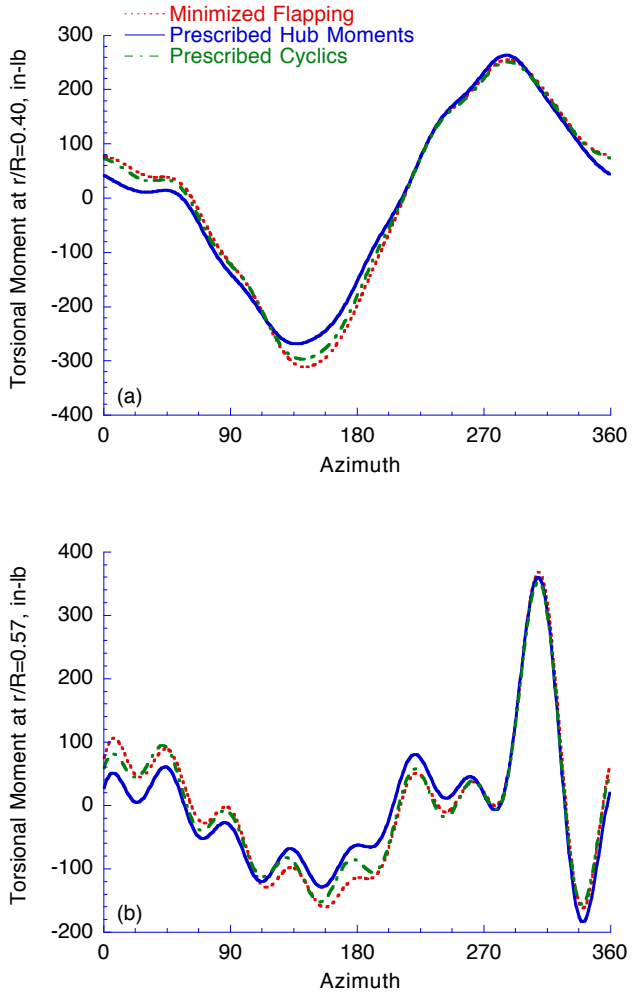

Figure 6. Comparison of oscillatory torsional moments with three procedures to setting on a test condition in the wind tunnel, a) torsional moment at r/R=0.40, b) torsional moment at r/R=0.57.

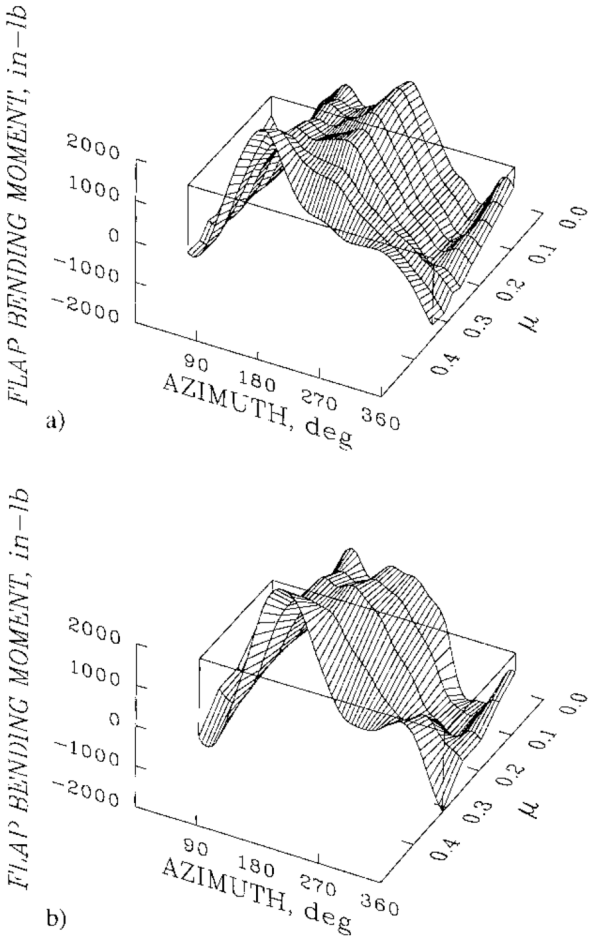

Figure 7. Comparison of wind tunnel and flight test oscillatory flap bending at r/R=0.144 as a function of advance ratio and azimuth position, a) flight test, b) wind tunnel test.

Figure 5 is a comparison of oscillatory chord bending moment time histories at two blade radial locations (r/R=0.144 and r/R=0.57) at the same test condition as Fig. 4, and for the same three approaches to setting on a test condition in the wind tunnel. Again, distinct differences are noted at the inboard radial station (r/R=0.144), between the procedure for setting up on prescribed hub moments and the procedures for minimized flapping or prescribed cyclics. As in Fig. 4a, these differences are almost entirely a function of the 1P control input for trim, with very little change in the higher frequency loading. The significant observation in Fig. 5a is the decrease in the oscillatory chordwise bending moment by approximately a factor of 2 with the prescribed hub moment trim approach relative to the minimized flapping trim approach. Unlike the flap bending moment comparison in the previous figure (Fig. 4b), small, but distinct differences in the measured chord bending moment are noted at the midspan (r/R=0.57) radial station.

Figure 6 is a comparison of oscillatory torsional moment time histories at two blade radial locations (r/R=0.40 and r/R=0.57) at the same test condition as Figs. 4 and 5, and for the same three approaches to setting on a test condition in the wind tunnel. Small differences are noted at the innermost radial station (r/R=0.40), primarily at azimuthal positions near the nose and tail of the RTA. Again small differences in the measured

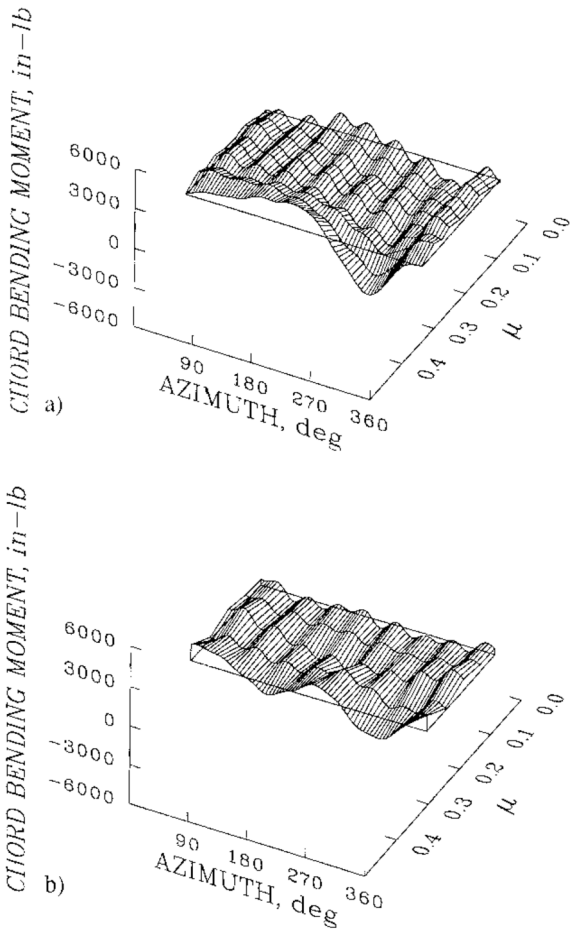

Figure 8. Comparison of wind tunnel and flight test oscillatory chord bending at r/R=0.144 as a function of advance ratio and azimuth position, a) flight test, b) wind tunnel test.

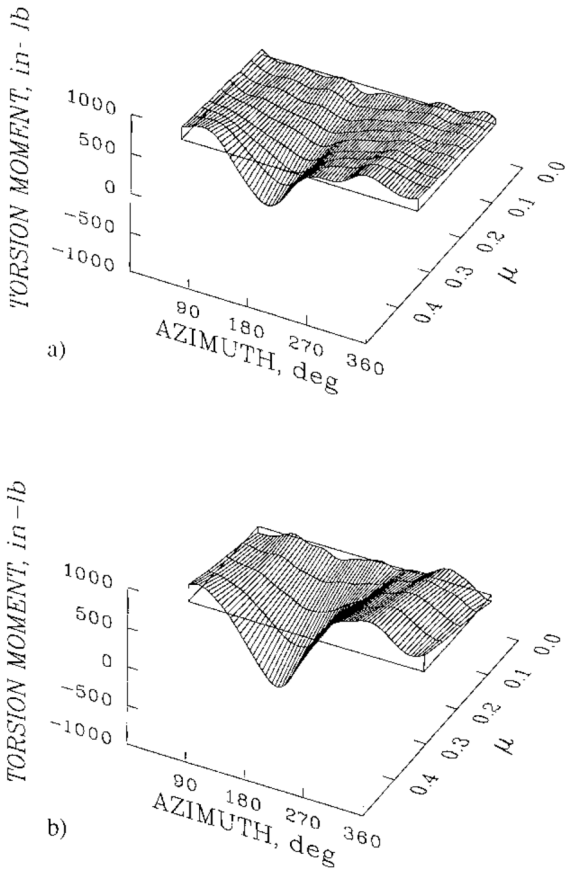

Figure 9. Comparison of wind tunnel and flight test oscillatory torsional moment at r/R=0.40 as a function of advance ratio and azimuth position, a) flight test, b) wind tunnel test.

torsional moment are noted at the midspan (r/R=0.57) radial station, primarily on the advancing side.

Wind Tunnel and Flight Comparisons

Figures 7-9 present an overall comparison of the wind tunnel data acquired with flight test data. All comparisons between wind tunnel and flight are with the prescribed hub moment trim procedure in the wind tunnel. Data are presented as a function of advance ratio and azimuth position for oscillatory (1-8 harmonics) flap and chord bending moments near the root of the blade (r/R=0.144) and for oscillatory torsional moments near midspan (r/R=0.40).

Figure 7 is a comparison of oscillatory flap bending moments at blade radius r/R=0.144 as a function of advance ratio and azimuth position. The overall comparisons between the flight test and the wind tunnel prescribed hub moment trim procedure is quite good.

Figure 8 is a comparison of the oscillatory chord bending moments at blade radius r/R=0.144 as a function of advance ratio and azimuth position. Again, the overall comparisons between the flight test and the wind tunnel prescribed hub moment trim procedure is quite good up to μ=0.25. However, noticeable differences can be seen at the higher advance ratios in the overall magnitude, with the flight test data showing the higher loading. Also, distinct differences in the character of the time histories between flight test and the wind tunnel can be seen for μ>0.25.

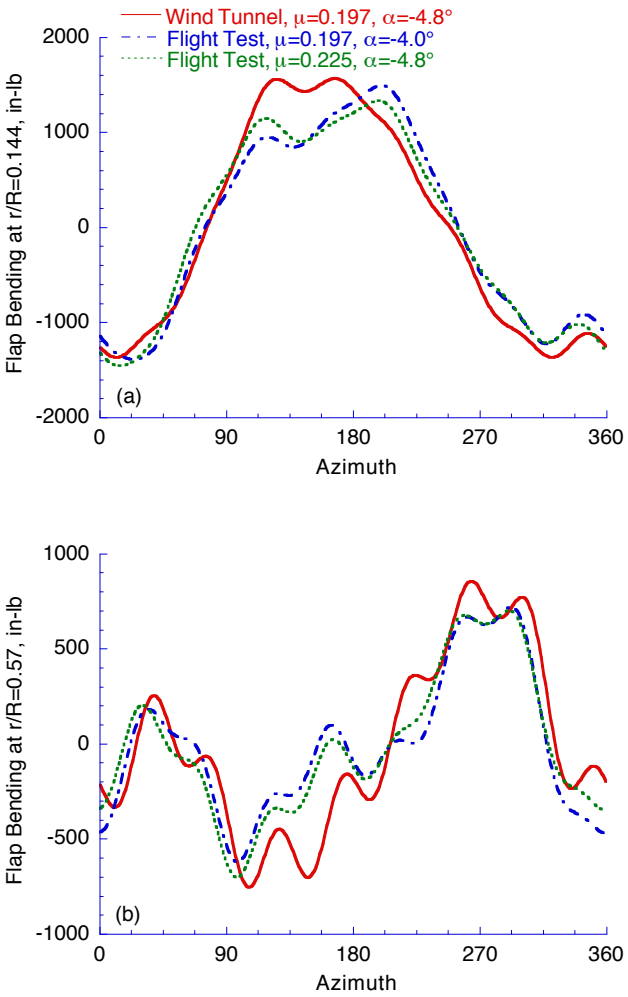

Figure 10. Comparison of wind tunnel and the two nearest flight test conditions, a) flap bending at r/R=0.144, b) flap bending at r/R=0.57.

Figure 9 is a comparison of the oscillatory torsional moments at blade radius r/R=0.40 as a function of advance ratio and azimuth position. Again, the comparisons between the flight test and the wind tunnel prescribed hub moment trim procedure is quite good. However, as in the chord bending comparison shown in Fig. 8, there are noticeable differences at the higher advance ratios in the overall magnitude, with in this case, the wind tunnel data showing the higher loading.

Table 4. Summary of wind tunnel and flight test conditions for Figs. 10-12.

	μ	α	C_{Mx}/σ	C_{My}/σ
Tunnel	0.197	-4.8°	-0.00053	0.00159
Flight	0.197	-4.0°	-0.00039	0.00155
Flight	0.225	-4.8°	-0.00054	0.00154

More detailed comparisons of wind tunnel and flight test data are presented in Figs. 10-15. Figures 10-12 compare wind tunnel and flight test oscillatory (1-8 harmonics) flap bending and chord bending and torsional moments for a moderate flight speed. Figures 13-15 compare wind tunnel and flight test oscillatory flap bending and chord bending and torsional moments for the highest flight speed tested (μ=0.313) for comparison in the wind tunnel. Because of the measured airspeed errors discussed previously, comparisons of flight test data with wind tunnel data are made with the two nearest flight test speeds. The differences between the two flight conditions and the wind tunnel test conditions are typically that one condition will match the advance ratio and the other condition will match the shaft angle of attack and the pitch and roll moments.

Figures 10-12 compare wind tunnel and flight test data for a nominal advance ratio of μ=0.197 and a shaft angle of attack of α=-4.8 deg. The two nearest flight conditions are for an advance ratio of μ=0.197 and -4.0 deg angle of attack, and for an advance ratio of μ=0.225 and -4.8 deg angle of attack. Corresponding hub moments for the wind tunnel and the two flight conditions are summarized in Table 4.

Figure 10 is a comparison of oscillatory flap bending at blade radial stations r/R=0.144 and r/R=0.57 (r/R=0.55 for the flight test) for both the wind tunnel and the corresponding flight test conditions at a nominal advance ratio of μ=0.197. The comparison at r/R=0.144 is quite good for the 1P loading, however the higher frequency loading, primarily the 2P and 3P magnitudes are different between the two tests. The differences in the higher frequency loading in this figure and those to follow are likely a result of aerodynamic differences between the RTA and the fuselage of the BO-105 aircraft. The comparison at the midspan radial station (r/R=0.57 and r/R=0.55) is also quite good in that the basic waveform was captured in the wind tunnel. There are however, subtle differences in the higher frequency loading between the wind tunnel test and the flight test data.

Figure 11 is a comparison of oscillatory chord bending at blade radial stations r/R=0.144 and r/R=0.45 for both the wind tunnel and the corresponding flight test conditions at a nominal advance ratio of μ=0.197. The comparison at r/R=0.144 shows similar loading in that the higher frequency (8P) loading appears to be approximately of the same magnitude and phase, but the

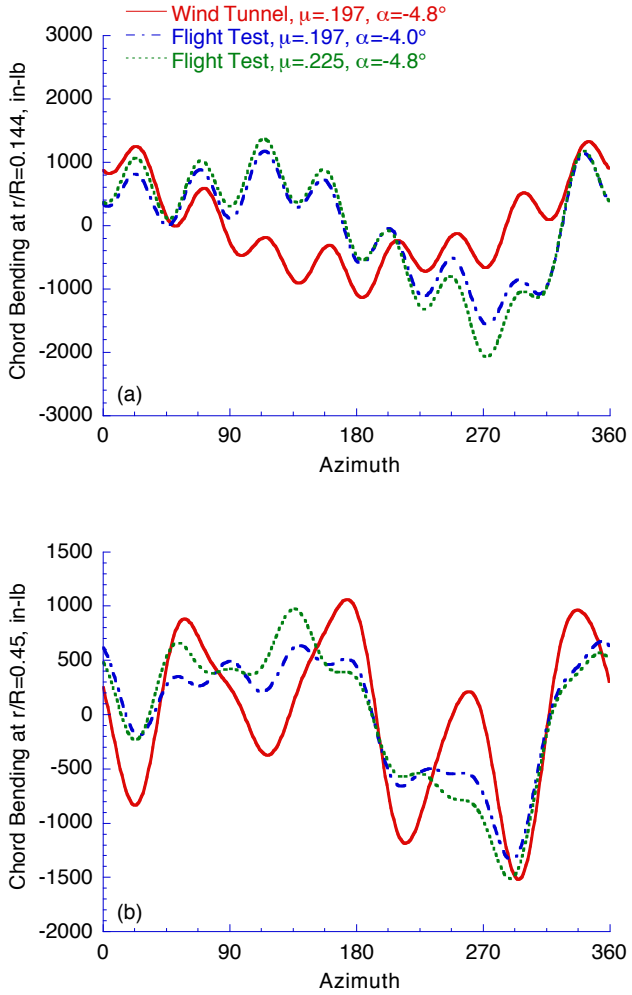

Figure 11. Comparison of wind tunnel and the two nearest flight test conditions, a) chord bending at r/R=0.144, b) chord bending at r/R=0.45.

low frequency loading is different primarily in phase. The comparison at the midspan radial station (r/R=0.45) also shows similar loading in that the basic waveform was captured in the wind tunnel. The difference between the wind tunnel and the flight test data is that the wind tunnel has a lower 1P loading, but a higher 4P loading.

Figure 12 is a comparison of oscillatory torsional moment at blade radial station r/R=0.40 for both the wind tunnel and the corresponding flight test conditions at a nominal advance ratio of μ=0.197. The comparison again shows similar loading in that the basic waveform was captured in the wind tunnel. The primary difference between wind tunnel and flight test is in the 1P and 2P loading. The differences in loading may be attributed to

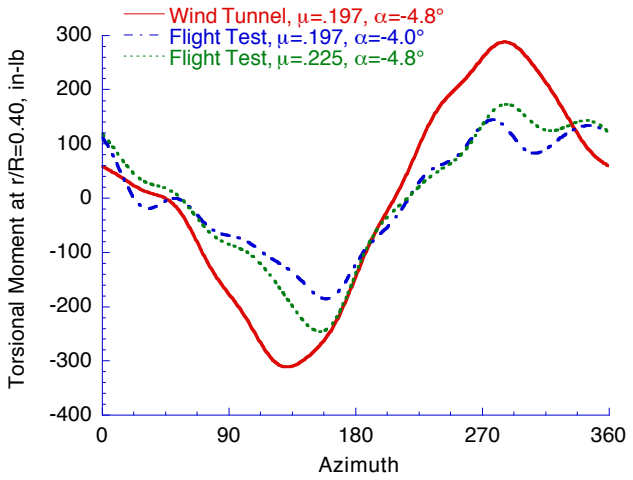

Figure 12. Comparison of wind tunnel and the two nearest flight test conditions, torsional moment at r/R=0.40.

the differences in both stiffness and arrangement of the control systems beginning at the pitch links.

Figures 13-15 compare wind tunnel and flight test data for a nominal advance ratio of μ=0.313 and a shaft angle of attack of α=-9.6 deg. The two nearest flight conditions are for an advance ratio of 0.306 and -7.7 deg angle of attack, and for an advance ratio of μ=0.341 and -9.6 deg angle of attack. Corresponding hub moments for the wind tunnel and the two flight conditions are summarized in Table 5.

Figure 13 is a comparison of oscillatory flap bending at blade radial stations r/R=0.144 and r/R=0.57 (r/R=0.55 for the flight test) for both the wind tunnel and the corresponding flight test conditions at a nominal advance ratio of μ=0.313. The comparison at r/R=0.144 is quite good for the 1P loading; however, the wind tunnel data exhibits a more pronounced 2P loading. The 2P loading of the flight test data is approximately half of the wind tunnel data at this test condition. The comparison at the

Table 5. Summary of wind tunnel and flight test conditions for Figs. 13-15.

	μ	α	C_{Mx}/σ	C_{My}/σ
Tunnel	0.313	-9.6°	-0.00102	0.00074
Flight	0.306	-7.7°	-0.00089	0.00148
Flight	0.341	-9.6°	-0.00112	0.00109

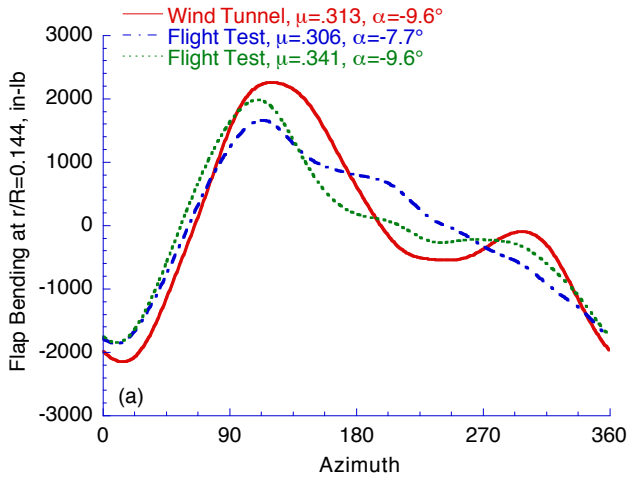

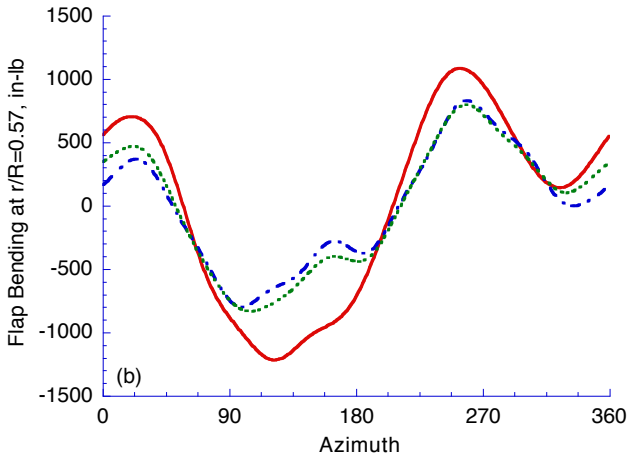

Figure 13. Comparison of wind tunnel and the two nearest flight test conditions, a) flap bending at r/R=0.144, b) flap bending at r/R=0.57.

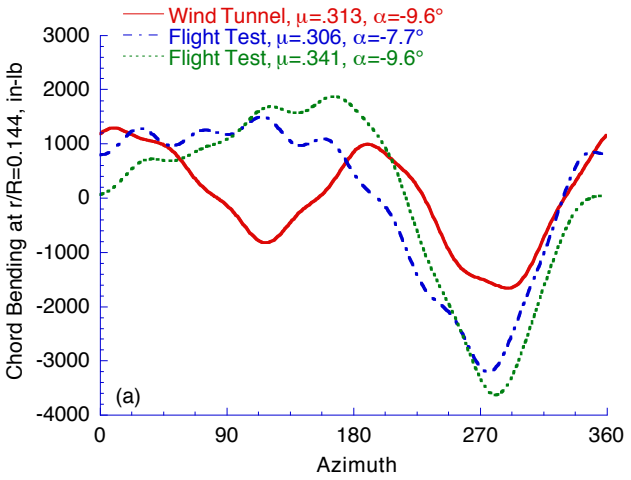

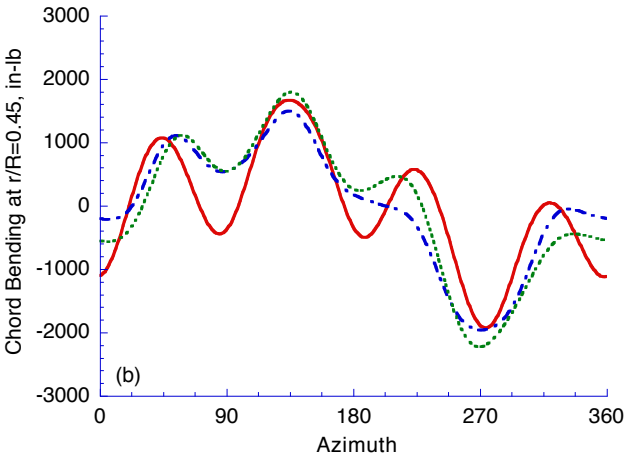

Figure 14. Comparison of wind tunnel and the two nearest flight test conditions, a) chord bending at r/R=0.144, b) chord bending at r/R=0.45.

midspan radial station (r/R=0.57 and r/R=0.55) is also quite good in that the basic waveform was captured in the wind tunnel. The differences between the wind tunnel and flight test data are primarily in the 1P and 2P loading.

Figure 14 is a comparison of oscillatory chord bending at blade radial stations r/R=0.144 and r/R=0.45 for both the wind tunnel and the corresponding flight test conditions at a nominal advance ratio of μ=0.313. The comparison at r/R=0.144 is again fair in that the relative phasing is similar, however the magnitude of the 1P loading in the wind tunnel is less than a third of that from the flight test. The wind tunnel data also exhibits a greater 2P loading than the flight test. The comparison at the midspan radial station (r/R=0.45) is again quite good in that the basic waveform was captured in the wind tunnel. As in Fig. 11b, the differences between the wind tunnel and the flight test data is that the wind tunnel has a lower 1P loading, but a higher 4P loading.

Figure 15 is a comparison of oscillatory torsional moment at blade radial station r/R=0.40 for both the wind tunnel and the corresponding flight test conditions at a nominal advance ratio of μ=0.313. The comparison is again fair, and is very similar to Fig. 12. The primary difference between wind tunnel and flight test data is in the 1P and 2P loading.

CAMRAD/JA Analysis

The CAMRAD/JA (Ref. 3) analysis code is used to obtain analytical predictions. CAMRAD/JA is a

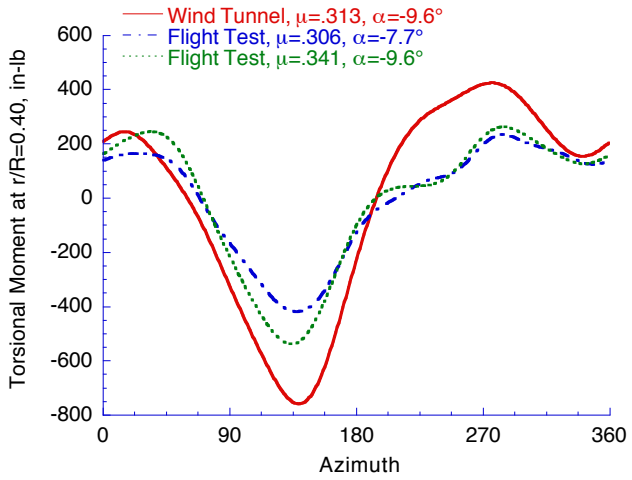

Figure 15. Comparison of wind tunnel and the two nearest flight test conditions, torsional moment at r/R=0.40.

comprehensive analytical model designed to calculate rotor performance, aerodynamic and structural loads, aircraft vibration, gust response, flight dynamics, handling qualities, and aeroelastic stability.

The rotor structural model within CAMRAD/JA is based on engineering beam theory for rotating wings with large pitch and pretwist. Both rigid and elastic blade motions are included. A single load path is assumed and the hingeless rotor blade is modeled as cantilevered beam with a straight, undeformed elastic axis. The definition of the rotor structural properties were provided to NASA and the U.S. Army, by EuroCopter Deutschland (formerly Messerschmitt-Bölkow-Blohm GmbH) and the Deutsche Forschungsanstalt für Luft-und Raumfahrt e.V. (DLR Institute for Flight Mechanics) under the auspices of the U.S. Army/German Memorandum of Understanding on Cooperative Research in the Field of Helicopter Aeromechanics. The key rotor blade cross-sectional structural modeling parameters are presented and discussed in Ref. 4.

The rotor aerodynamic model within CAMRAD/JA is based on second-order, lifting-line theory and uses steady, two-dimensional airfoil characteristics, with corrections for unsteady and three-dimensional flow effects. Included in CAMRAD/JA is the option to use uniform inflow (linear variation of inflow over the rotor disk), nonuniform inflow with a prescribed wake geometry, or nonuniform inflow with a free wake geometry in the solution procedure. The freewake model was used in the correlation study.

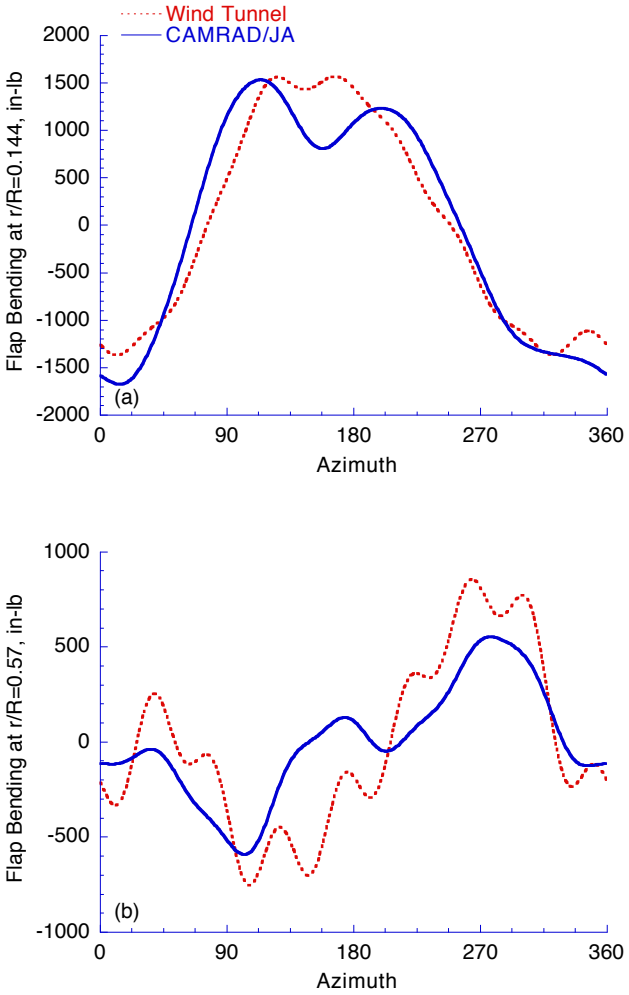

Figure 16. Correlation of CAMRAD/JA results with measured wind tunnel data, a) flap bending at r/R=0.144, b) flap bending at r/R=0.57.

Correlation Results

Correlation results with measured wind tunnel data and CAMRAD/JA are presented in Figs. 16-21. Results are presented for the prescribed hub moment approach to setting on condition in the wind tunnel for two different advance ratios (μ=0.197 and 0.313) at the 1-g thrust condition (C_T/σ=0.07). In the analysis, the rotor was trimmed to the measured 1P root flapping moment (r/R=0.144) of blade number three. As previously mentioned, blade number three was chosen as the representative blade after careful review of wind tunnel data relative to the flight test, and correlation with analysis. Correlation results are presented for oscillatory (1-8 harmonics) flap and chord bending near the blade root (r/R=0.144) and near midspan (r/R=0.57).

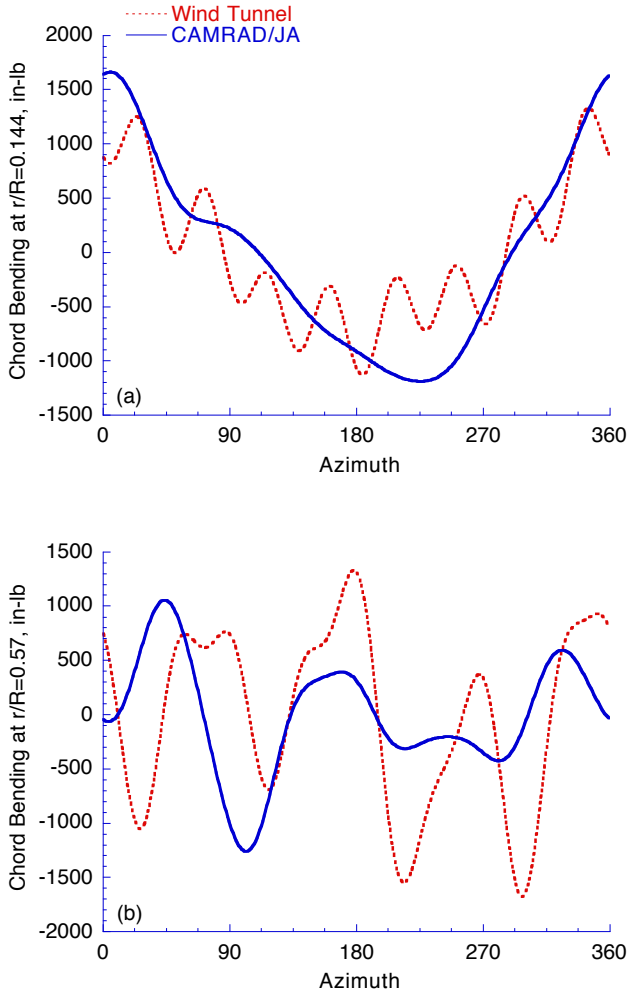

Figure 17. Correlation of CAMRAD/JA results with measured wind tunnel data, a) chord bending at r/R=0.144, b) chord bending at r/R=0.57.

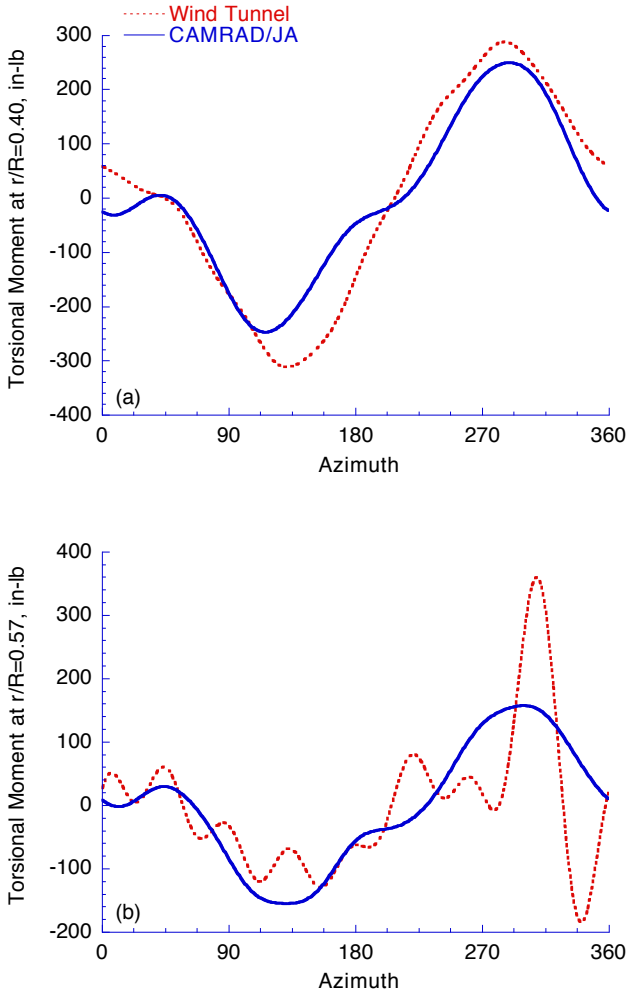

Figure 18. Correlation of CAMRAD/JA results with measured wind tunnel data, a) torsional moment at r/R=0.40, b) torsional moment at r/R=0.57.

Correlation results for oscillatory (1-8 harmonics) torsional moment is presented for two locations near midspan (r/R=0.40 and r/R=0.57).

Figure 16 is a comparison of CAMRAD/JA with wind tunnel measurements for an advance ratio of μ=0.197 and 1-g thrust at two blade radial stations. Figure 16a is a comparison of oscillatory flap bending at r/R=0.144. The 1P component of the flap moment was prescribed by the trim procedure and therefore the correlation of flapping is excellent. However, CAMRAD/JA predicts more 2P and 3P flapping than was actually measured in the wind tunnel. Figure 16b is a comparison of CAMRAD/JA with wind tunnel results for a midspan radial station, r/R=0.57. CAMRAD/JA captures the basic waveform of the measured test results, however it does not accurately predict the higher frequency (primarily 2P and 8P) loading.

Figure 17 is a comparison of CAMRAD/JA with wind tunnel results for the same test conditions as in Fig. 16. Figure 17a is comparison of oscillatory chord bending at r/R=0.144. The comparison for chord bending is good in that the basic waveform was captured; however again, CAMRAD/JA does not accurately predict the higher frequency (primarily 8P) loading. Figure 17b is a comparison at a midspan radial station, r/R=0.57. The correlation of CAMRAD/JA with wind tunnel results is poor at this radial station. The qualitative nature of the loading is not captured in this analysis; however, one might call the correlation fair judging by the similar peak-to-peak magnitude of the oscillatory loading.

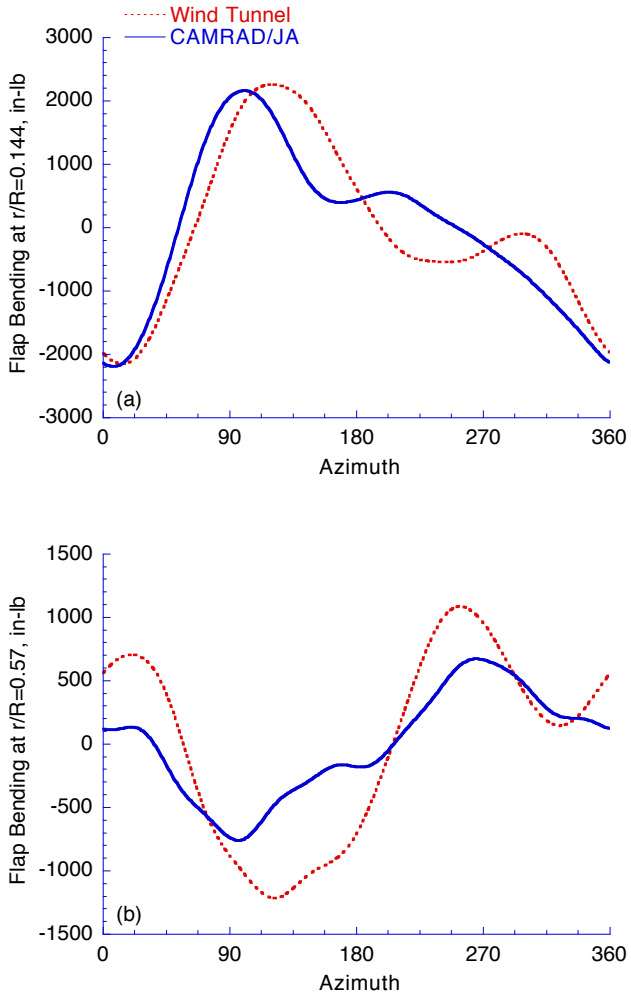

Figure 19. Correlation of CAMRAD/JA results with measured wind tunnel data, a) flap bending at r/R=0.144, b) flap bending at r/R=0.57.

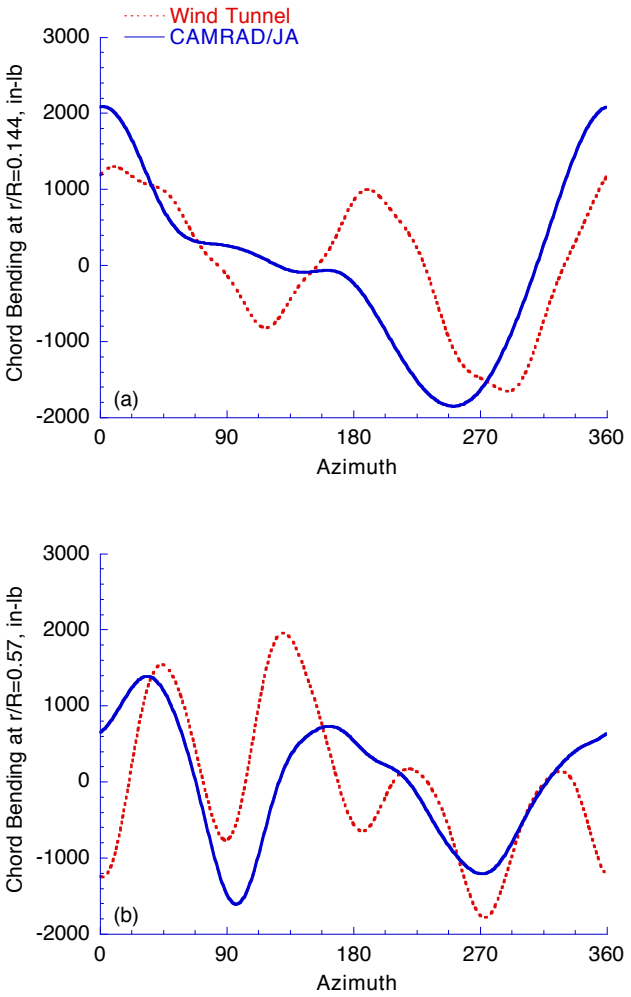

Figure 20. Correlation of CAMRAD/JA results with measured wind tunnel data, a) chord bending at r/R=0.144, b) chord bending at r/R=0.57.

Figure 18 is a comparison of CAMRAD/JA with wind tunnel results for the same test conditions as in Figs. 16-17. Figure 18a is comparison of oscillatory torsional moment at r/R=0.40. The comparison for torsional moment is quite good. Figure 18b is a comparison at a radial station (r/R=0.57) closer to midspan. CAMRAD/JA predicts the basic waveform, but does not accurately predict the higher frequency (primarily 4P and 8P) loading.

Figure 19 is a comparison of CAMRAD/JA with wind tunnel results for an advance ratio of μ=0.313 and 1-g thrust at two blade radial stations. Figure 19a is comparison of oscillatory flap bending at r/R=0.144. As in Fig. 16a, the comparison for flap bending is good, as the analysis was trimmed to the 1P flapping moment as measured in the wind tunnel. However, CAMRAD/JA predicts less 2P and more 3P flapping than was actually measured in the wind tunnel. Figure 19b is a comparison at a midspan radial station, r/R=0.57. CAMRAD/JA captures the basic waveform of the measured test results, however it underpredicts the measured 2P and 3P flapping.

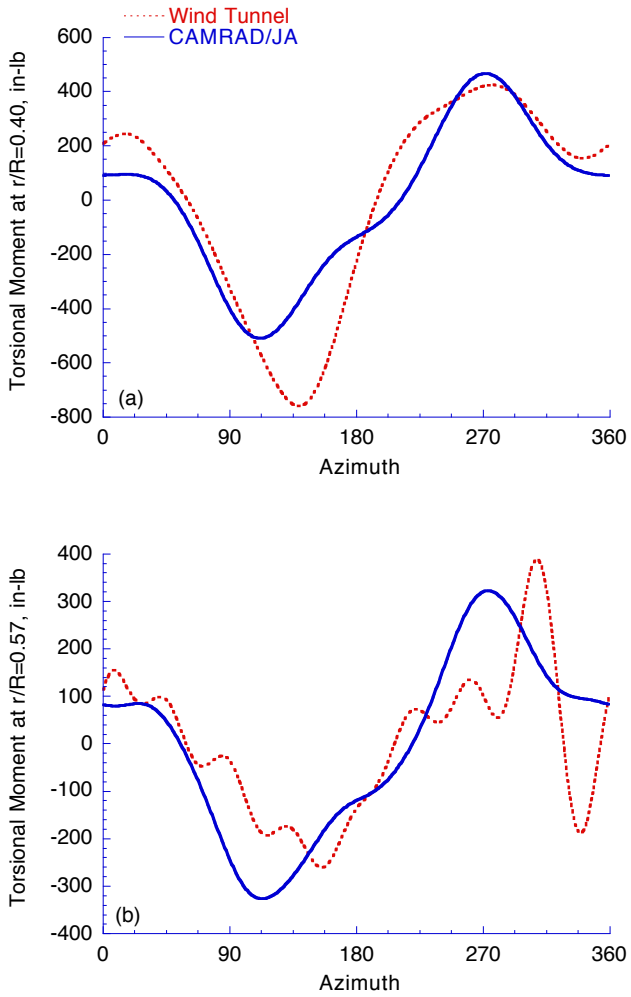

Figure 21. Correlation of CAMRAD/JA results with measured wind tunnel data, a) torsional moment at r/R=0.40, b) torsional moment at r/R=0.57.

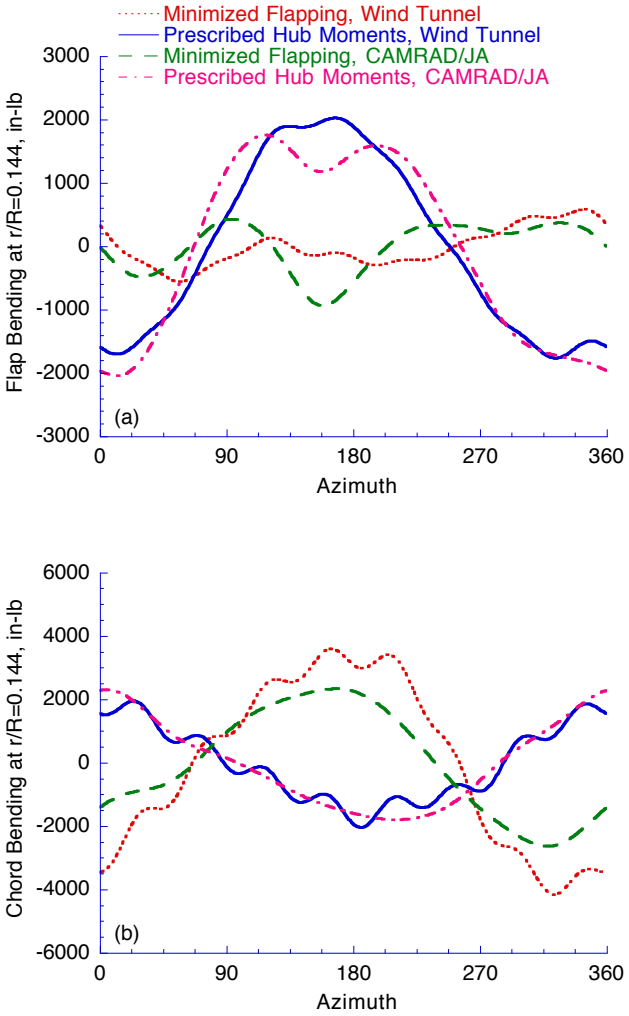

Figure 22. Correlation of CAMRAD/JA oscillatory bending moment results with wind tunnel data for minimized flapping and prescribed hub moment trim, a) flap bending at r/R=0.144, b) chord bending at r/R=0.144.

Figure 20 is a comparison of CAMRAD/JA with wind tunnel results for the same test conditions as in Fig. 19. Figure 20a is comparison of oscillatory chord bending at r/R=0.144. The comparison for chord bending is fair in that the overall magnitude was captured, however CAMRAD/JA does not predict the 1P loading seen in the wind tunnel test data. Figure 20b is a comparison at a midspan radial station, r/R=0.57. The correlation of CAMRAD/JA with wind tunnel results is again poor at this radial station as in Fig. 17b.

Figure 21 is a comparison of CAMRAD/JA with wind tunnel results for the same test conditions as in Figs. 19-20. Figure 21a is comparison of oscillatory torsional moment at r/R=0.40. The comparison for torsional moment is good; however the wind tunnel results contain more 2P and 3P loading. Figure 21b is a comparison at a radial station (r/R=0.57) closer to midspan. Again, CAMRAD/JA predicts the basic waveform, but does not accurately predict the higher frequency (primarily 4P and 8P) loading.

Analytic tools gain acceptance by the designers only after they have been proven to predict measured loads. It is especially important for rotorcraft analyses to correctly model physical phenomenon which result in large changes in hub and blade loads. It was seen in Fig. 5 that the root chord bending load changed dramatically when cyclic pitch inputs were changed for a given thrust, airspeed, and shaft angle. The ability of CAMRAD/JA to

predict this loading is shown in Fig. 22. The data presented is for the minimized flapping and prescribed hub moment approaches to setting on condition at an advance ratio of μ=0.197. In this figure, the experimental data is for blade number one and the CAMRAD/JA analysis was trimmed to the measured 1P flap bending moments. Figure 22a compares measured flap loads with those predicted with CAMRAD/JA. The calculated flap loads are adequate for design, but this is mainly a result of prescribing the 1P loads in the trim procedure. The resulting chord loads are shown in Figure 22b. CAMRAD/JA does reasonably well at predicting the large phase shift in the 1P loading due to the trim change, however, it does not do well at predicting the change in 1P magnitude. The CAMRAD/JA prediction of the change in peak-to-peak chord load due to the change in trim conditions is not adequate for design. The reason for this deficiency is not known at this time, but it clearly deserves further attention.

Concluding Remarks

Results from a correlation study of wind tunnel test of a full-scale four-bladed hingeless rotor system with flight test measurements were presented. Good correlation of measured blade root flap bending moments in the wind tunnel with flight test measurements was shown when the rotor was trimmed to measured flight test hub pitching and rolling moments. Analytical results using the CAMRAD/JA analysis showed good correlation with measured wind tunnel data for isolated rotor root flapping trim.

Comparison of Experimental Data

The ability to set up on measured flight test hub moments in the wind tunnel using the RTA balance was successfully demonstrated in this test program.

The type of trim procedure used to set on condition in the wind tunnel is important for the inboard flap bending, chord bending and torsion loads on hingeless rotors and for the outboard chord bending loads on the blade as well.

Reasonably good correlation between flight test and wind tunnel data for oscillatory flap and chord bending moments was shown despite small differences in advance ratio and angle of attack.

Comparison with Analysis

CAMRAD/JA was able to predict reasonably well the low frequency blade loading when trimmed to the measured 1P flapping moments.

CAMRAD/JA was unable to predict the higher frequency loading as measured in the wind tunnel and in flight.

CAMRAD/JA was able to predict reasonably well the phase change of the blade root oscillatory chord bending for two different approaches to setting on condition in the wind tunnel. The change in the 1P magnitude between the two approaches was not predicted by CAMRAD/JA.

References

[1] Langer, H. J. and Tränapp, N, "BO105 Flight Test Data For A Wind Tunnel Test Program," Deutsche Forschungsanstalt für Luft- und Raumfahrt e.V., DLR-IB111-93/58, Institut für Flugmechanik, Braunschweig, Germany, Sept 1993.

[2] Staley, J. A., "Validation of Rotorcraft Flight Simulation Program through Correlation with Flight Data for Soft In-Plane Hingeless Rotors," USAAMRDL TR-75-50, Jan 1976.

[3] Johnson, W., "A Comprehensive Analytical Model of Rotorcraft Aerodynamics and Dynamics, Theory Manual, Johnson Aeronautics Version," Johnson Aeronautics, 1989.

[4] Peterson, R. L. and Johnson, W., "Aeroelastic Loads and Stability Investigation of a Full-Scale Hingeless Rotor," *Proceedings of the International Forum on Aeroelasticity and Structural Dynamics*, Aachen, Germany, Jun 1991.